Brain Segmentation from 3D MRI Using Statistically Learned Physics-Based Deformable Models

Christophoros NIKOU[1,2], Fabrice HEITZ[1], Jean-Paul ARMSPACH[2]

[1] Laboratoire des Sciences de l'Image de l'Informatique et de la Télédétection,
CNRS UPRES-A 7005/Strasbourg I University,
4 bd. Sébastien Brant, 67400 Illkirch, France
nikou@mondrian.u-strasbg.fr, Fabrice.Heitz@ensps.u-strasbg.fr

[2] Institut de Physique Biologique, Faculté de Médecine,
CNRS UPRES-A 7004/Strasbourg I University,
4 rue Kirschleger, 67085 Strasbourg, France
armspach@alsace.u-strasbg.fr

Abstract

In this paper, we introduce a statistical deformable model for the segmentation of the brain structure in 3D MRI. Our approach relies on a physically deformable multimodel that embeds information on head (skull and scalp) and brain by parameterizing these structures by the amplitudes of vibration of an initial spherical mesh. The spatial relation between head and brain is then statistically learned through an off-line training procedure using a representative population of 3D MRI. In order to segment the brain from a MR image not belonging to the training set, we first segment the head surface. The brain contour coordinates are then iteratively recovered using their statistical relations to the head coordinates.

I. Introduction

Since the seminal work of Kass *et al.* [1] on 2D shape models, deformable models have gained increasing popularity in computer vision to segment, match or track rigid and nonrigid objects [2, 3, 4, 5, 6, 7, 8]. In medical image analysis, deformable models offer a unique and powerful approach to accommodate the significant variability of biological structures over time and across different individuals. A survey on deformable models as a promising computer-assisted medical image analysis technique may be found in [9].

Among the different segmentation methods, deformable model-based segmentation relies on rigid or deformable models of the structures (usually regions, surfaces or curves) of interest. Statistical deformable models [3, 4, 10], in particular, are good candidate for representing the statistical variability of anatomical structures. In [11], for instance, a multislice 2D point distribution model (PDM) [3] is deformed to match various structures in single modal PET images. More recently, 3D physically-based deformable models constrained by statistical analysis have also been applied to characterize pathological shape deformations in [12].

In this paper, we introduce a deformable model-based approach for the segmentation of the brain structure in 3D MRI. Our approach relies on a learned deformable multimodel that embeds information about the different anatomical structures that are to be extracted from the MRI. The different model parts are statistically constrained to represent the structures of interest and their spatial relationships. These constraints are learned from a representative population in an off-line training procedure. This approach is applied here by modeling the head (skull and scalp) and brain contours in the MR images. As the head structure can easily be segmented from the MR volume, the brain contour coordinates may be recovered reliably using their statistical (anatomical) relationship to the head coordinates, as explained in the following.

II. A statistically learned multiobject deformable model

To provide a training set, a representative collection of 3D MRI volumes of different patients have first been registered to a reference image using an unsupervised robust registration technique developed by the authors [13, 14]. The head of each volume has then been segmented by simple thresholding [15] and region growing. The brain has also been segmented by a semi-manual technique consisting of thresholding and region growing [16]. Both head and brain contours have then been parameterized by the amplitudes of the vibration modes of a deformable spherical mesh [5] by solving the system evolution equation:

$$\mathbf{M}\ddot{\mathbf{U}}(t) + \mathbf{C}\dot{\mathbf{U}}(t) + \mathbf{K}\mathbf{U}(t) = \langle \mathbf{F}(t), \vec{\mathcal{N}} \rangle \vec{\mathcal{N}} \qquad (1)$$

where $\mathbf{M}$, $\mathbf{C}$, $\mathbf{K}$ are the mass, dumping and stiffness matrix of the system, $\mathbf{U}$ stands for the nodal displacements, $\mathbf{F}$ is the image force at each node of the spherical mesh, which is projected on vector $\vec{\mathcal{N}}$ which is normal to the surface at each node, in order to capture fine details of the contour. The image force $\mathbf{F}(t)$ at each pixel is the chamfer distance between the image point and its nearest contour point [17].

0-7803-5021-9/99/$10.00 © 1999 IEEE.

Equation (1) is of order $3N$, where N is the total number of nodes of the spherical mesh. It is solved in the subspace of the vibration modes [5] using the following change of basis vectors:

$$\mathbf{U} = \mathbf{\Phi}\tilde{\mathbf{U}} = \sum_i \tilde{u}_i \phi_i, \tag{2}$$

where $\mathbf{\Phi}$ is a matrix and $\tilde{\mathbf{U}}$ is a vector, ϕ_i is the i^{th} row of $\mathbf{\Phi}$ and $\tilde{u}$ is a scalar. By choosing $\mathbf{\Phi}$ as the matrix whose columns are the eigenvectors of the eigenproblem:

$$\mathbf{K}\phi_i = \omega_i^2 \mathbf{M}\phi_i, \tag{3}$$

$\mathbf{M}$ and $\mathbf{K}$ are simultaneously diagonalized and the system (1) is simplified to $3N$ scalar equations [5]:

$$\ddot{\tilde{u}}_i(t) + \tilde{c}_i \dot{\tilde{u}}_i(t) + \omega_i^2 \tilde{u}_i(t) = \tilde{f}_i(t). \tag{4}$$

In equation (4), ω_i designates the i^{th} eigenvalue of equation (3), $\tilde{u}_i$ is the amplitude of the corresponding vibration mode, $\tilde{c}_i$ are the nonzero (diagonal) elements of

$$\tilde{\mathbf{C}} = \mathbf{\Phi}^T \mathbf{C} \mathbf{\Phi} \tag{5}$$

and

$$\tilde{f}_i(t) = \mathbf{\Phi}^T [\langle \mathbf{F}(t), \vec{\mathcal{N}} \rangle \vec{\mathcal{N}}]. \tag{6}$$

The nondiagonal elements of $\tilde{\mathbf{C}}$ are zero because we have simplified the dumping matrix of the system by assuming that the dumping matrix $\mathbf{C}$ is constructed using the Caughey series [18]:

$$\mathbf{C} = \mathbf{M} \sum_{k=0}^{p-1} \alpha_k [\mathbf{M}^{-1}\mathbf{K}]^k \tag{7}$$

For $k = 2$, equation (7) reduces to Rayleigh dumping [19]:

$$\mathbf{C} = \alpha_0 \mathbf{M} + \alpha_1 \mathbf{K} \tag{8}$$

and equation (5) provides us with the diagonal matrix:

$$\tilde{\mathbf{C}} = \alpha \mathbf{I} + \beta \mathbf{\Omega} \tag{9}$$

where $\mathbf{I}$ is the identity matrix and $\mathbf{\Omega}$ is the diagonal matrix whose elements are the eigenvalues ω_i.

For each image pair i in the training set, a vector $\mathbf{a}_i$ containing the N' most important vibration modes describing the head ($\tilde{\mathbf{u}}_i^h$) and the N'' most important vibration modes describing the brain ($\tilde{\mathbf{u}}_i^b$) is then created:

$$\mathbf{a}_i = (\tilde{\mathbf{u}}_i^h, \tilde{\mathbf{u}}_i^b)^T \tag{10}$$

where:

$$\tilde{\mathbf{u}}_i^h = (\tilde{u}_1^h, \tilde{u}_2^h, \ldots, \tilde{u}_{N'}^h)_i \tag{11}$$

$$\tilde{\mathbf{u}}_i^b = (\tilde{u}_1^b, \tilde{u}_2^b, \ldots, \tilde{u}_{N''}^b)_i \tag{12}$$

with $3(N' + N'') < 6N$.

Random vector $\mathbf{a}_i$ is then statistically constrained by retaining the most significant variation modes in its Karhunen-Loeve (KL) transform [3, 4, 20]:

$$\mathbf{a}_i = \bar{\mathbf{a}} + \mathbf{P}\mathbf{b}_i \tag{13}$$

where

$$\bar{\mathbf{a}} = \frac{1}{n} \sum_{i=1}^{n} \mathbf{a}_i \tag{14}$$

is the average vector of vibration amplitudes of the structures belonging to the training set, $\mathbf{P}$ is the matrix whose columns are the eigenvectors of the covariance matrix

$$\mathbf{\Gamma} = \mathbb{E}[(\mathbf{a}_i - \bar{\mathbf{a}})^T (\mathbf{a}_i - \bar{\mathbf{a}})] \tag{15}$$

and

$$\mathbf{b}_i = \mathbf{P}^T (\mathbf{a}_i - \bar{\mathbf{a}}) \tag{16}$$

are the coordinates of $(\mathbf{a}_i - \bar{\mathbf{a}})$ in the eigenvector basis.

The deformable model (corresponding to the head and brain contours) is finally parameterized by the m most significant statistical deformation modes stacked in vector $\mathbf{b}$. By modifying $\mathbf{b}$, both the head and the brain are deformed (fig. 1), according to the anatomical variability observed in the training set. Given the double initial spherical mesh

$$\bar{\mathbf{X}} = \begin{pmatrix} \bar{\mathbf{X}}_H \\ \bar{\mathbf{X}}_B \end{pmatrix} \tag{17}$$

where

$$\bar{\mathbf{X}}_H = (x_1^h, y_1^h, z_1^h, \ldots, x_{N'}^h, y_{N'}^h, z_{N'}^h)^T \tag{18}$$

$$\bar{\mathbf{X}}_B = (x_1^b, y_1^b, z_1^b, \ldots, x_{N''}^b, y_{N''}^b, z_{N''}^b)^T \tag{19}$$

the deformable multimodel $\mathbf{X}(\mathbf{b})$ is thus represented by:

$$\mathbf{X}(\mathbf{b}) = \bar{\mathbf{X}} + \mathbf{\Phi}\bar{\mathbf{a}} + \mathbf{\Phi}\mathbf{P}\mathbf{b} \tag{20}$$

where

$$\mathbf{\Phi} = \begin{pmatrix} \mathbf{\Phi}_H & \mathbf{0} \\ \mathbf{0} & \mathbf{\Phi}_B \end{pmatrix}, \quad \mathbf{P} = \begin{pmatrix} \mathbf{P}_{HB} \\ \mathbf{P}_{BH} \end{pmatrix} \tag{21}$$

and

$$\bar{\mathbf{a}} = \begin{pmatrix} \bar{\mathbf{a}}_H \\ \bar{\mathbf{a}}_B \end{pmatrix} \tag{22}$$

In equation (21), the columns of the $3N \times 3N'$ matrix $\mathbf{\Phi}_H$ are the eigenvectors of the spherical mesh describing the head surface and the columns of the $3N \times 3N''$ matrix $\mathbf{\Phi}_B$ are the eigenvectors of the spherical mesh describing the brain surface. Besides, the $3N' \times m$ matrix $\mathbf{P}_{HB}$ and the $3N'' \times m$ matrix $\mathbf{P}_{BH}$ describe the statistical dependences of head and brain vibration amplitudes observed in the training set. Vectors $\bar{\mathbf{a}}_H$ and $\bar{\mathbf{a}}_B$ are of order $3N' \times 1$ and $3N'' \times 1$ respectively, and vector $\mathbf{b}$ has a low dimension $m \ll 3(N' + N'')$. In our preliminary implementation, typical values are $N \simeq 20000$, $N' \simeq N'' \simeq \frac{N}{4} \simeq 5000$ and $m \simeq 10$. As it can be seen, thanks to the KL representation, only a few parameters ($m \simeq 10$) are necessary to describe the variations of the deformable model.

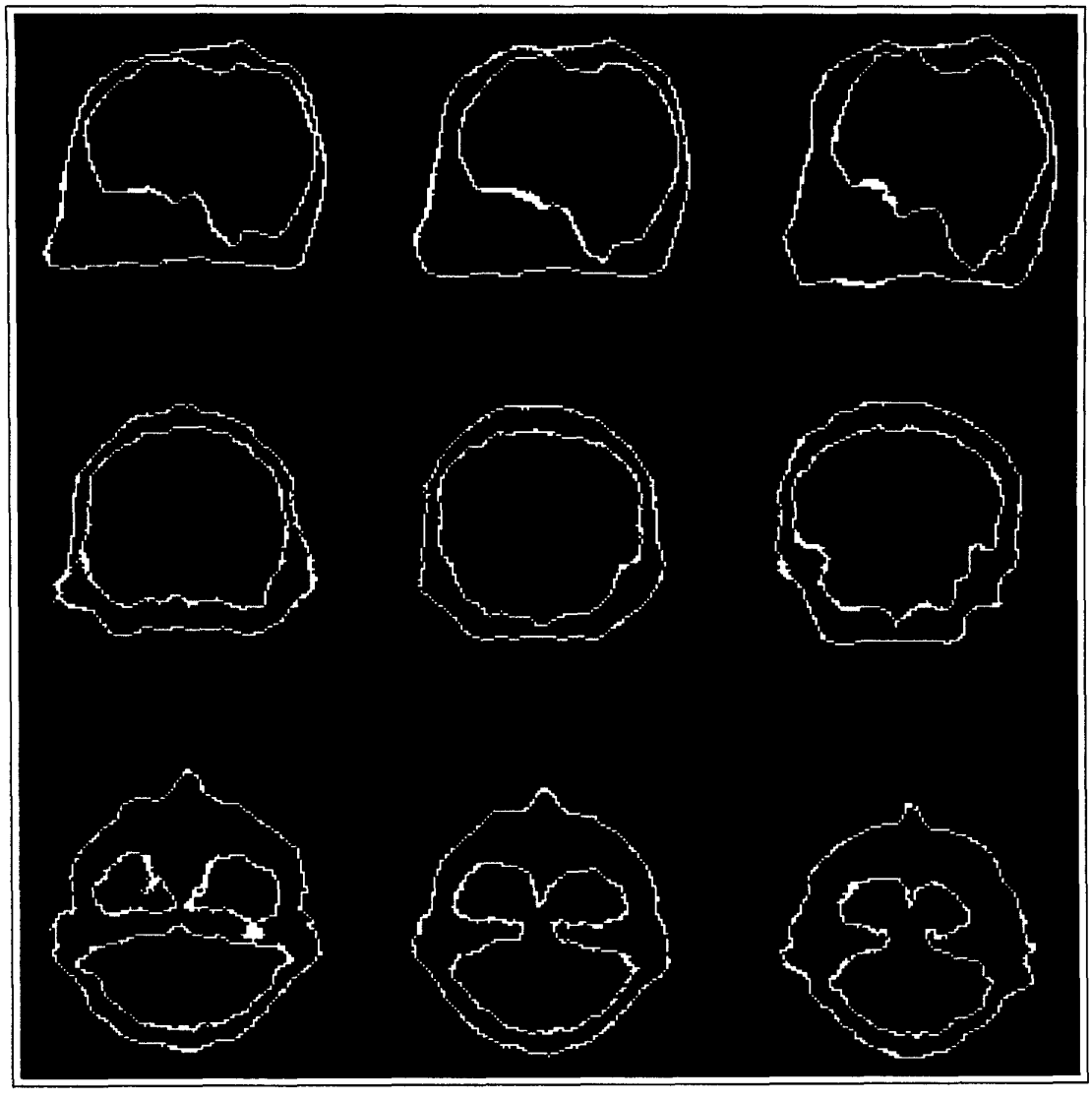

$\mathbf{b}[1] = -\sqrt{\lambda_1}$ $\mathbf{b}[1] = 0$ $\mathbf{b}[1] = \sqrt{\lambda_1}$

Figure 1: *Deformations of a 3D multimodel by varying the first statistical mode in vector* $\mathbf{b}$ *between* $-\sqrt{\lambda_1}$ *and* $\sqrt{\lambda_1}$. λ_1 *designates the first eigenvalue of the covariance matrix* $\mathbf{\Gamma}$. *Each column shows a multiplanar (sagittal, coronal, transversal) view of the 3D model.*

III. Brain segmentation

In order to extract the brain structure from a patient MRI volume not belonging to the training set, we first represent its head contour (that has been easily extracted by simple thresholding) by the amplitudes of the vibration modes of $\bar{\mathbf{X}}_H$. The head contour coordinates are then stacked in a vector $\mathbf{X}_H$. We solve equation (20) in the reduced space corresponding to the head coordinates only, to obtain a first least-squares estimate for vector $\mathbf{b}$ that matches the observed head contour:

$$\mathbf{b} = [(\mathbf{\Phi}_H\mathbf{P}_{HB})^T\mathbf{\Phi}_H\mathbf{P}_{HB}]^{-1}(\mathbf{\Phi}_H\mathbf{P}_{HB})^T (\mathbf{X}_H - \bar{\mathbf{X}}_H - \mathbf{\Phi}_H\bar{\mathbf{a}}_H). \quad (23)$$

Let us notice that the above solution is constrained by the matrix $\mathbf{P}_{HB}$ which relates the brain contour to the head contour coordinates, as learned from the training set. Equation (23) provides thus also *a good initial estimation of the location of the brain contour.*

Further improvement of this initial solution may be obtained by alternately optimizing an energy function

parameterized by the m components of vector $\mathbf{b}$ [4], in order to fit the part of the model describing the brain to a noisy contour map I_c extracted from the image [21] (fig. 2c). In our case, the cost function E to be optimized is defined as:

$$E = \sum_{i \in \mathbf{X}_B | i=1}^{N''} I_c(\mathbf{X}_B(\mathbf{b})) \quad (24)$$

The above equation counts the number of points of the model located on a contour point.

To summarize, the overall segmentation algorithm is based on the following steps:

- Computation of the statistical deformation parameters $\mathbf{b}$ by solving the overconstrained system (23).
- Prediction of the brain surface by equation (20).
- Fine-tuning of the solution by deterministic optimization of the cost function (24).

The whole segmentation process takes about 20 min cpu time on a HP C200 workstation for a 128^3 image volume. Figure 3 illustrates a preliminary exemple of segmentation obtained with this technique.

IV. Conclusion

We have presented a statistical deformable model-based technique for the segmentation of the brain structure in 3D MRI. Thanks to the statistical constraints embedded in the deformable model, the method should be robust and it could be applied to the segmentation of the brain structure from post operative images where missing anatomical structures lead standard voxel-based techniques to erroneous segmentations. This aspect is a perspective of our study.

The method is not limited to MRI brain segmentation but it may be adapted to other image modalities and/or to other anatomical structures or functional information. The described approach is also a first step towards the creation of an anatomical atlas that may be used for brain segmentation, intrasubject and intersubject registration.

Acknowledgments

This study has been supported by the Commission of the European Communities, DG XII, in the framework of the TMR program (Training and Mobility of Researchers), contract No ERBFMIBCT960701 and by the "Groupement d'Intérêt Scientifique-Sciences de la Cognition" (CNRS, CEA, INRIA, MENESR).

V. References

[1] M. Kass, A. Witkin, and D. Terzopoulos, "Snakes: active contour models," *International Journal of Computer Vision*, vol. 4, no. 1, pp. 321–331, 1988.

[2] G.E. Christensen, M.I. Miller, M.W. Vannier, and U. Grenander, "Individualizing neuro-anatomical atlases using a massively parallel computer," *IEEE Computer*, pp. 32–38, January 1996.

[3] T. F. Cootes, C. J. Taylor, and J. Graham, "Active shape models - their training and application," *Computer Vision and Image Understanding*, vol. 1, no. 1, pp. 38–59, 1995.

[4] C. Kervrann and F. Heitz, "A hierarchical Markov modeling approach for the segmentation and tracking of deformable shapes," *Graphical Models and Image Processing*, vol. 60, no. 3, pp. 173–195, 1998.

[5] C. Nastar and N. Ayache, "Frequency-based nonrigid motion analysis," *IEEE Transactions on Pattern Analysis and Machine Intelligence*, vol. 18, no. 11, pp. 1069–1079, 1996.

[6] R. Bajcsy and S. Kovačič, "Multiresolution elastic matching," *Computer Vision, Graphics and Image Processing*, vol. 46, pp. 1–21, 1989.

[7] C. Davatzikos, "Spatial transformation and registration of brain images using elastically deformable models," *Computer Vision and Image Understanding*, vol. 66, no. 2, pp. 207–222, 1997.

[8] C. Kervrann and F. Heitz, "Statistical model-based segmentation of deformable motion.," in *Proceedings of the 3rd IEEE International Conference on Image Processing (ICIP '96)*, Lausanne, Switzerland, 1996, pp. 937–940.

[9] T. Mc Inerney and D. Terzopoulos, "Deformable models in medical image analysis: a survey," *Medical Image Analysis*, vol. 2, no. 1, pp. 91–108, 1996.

[10] U. Grenader and M. I. Miller, "Representation of knowledge in complex systems," *Journal of the Royal Statistical Society*, vol. 56, no. 3, pp. 1994, 1994.

[11] C. L. Huang, W. T. Chang, L. C. Wu, and J. K. Wang, "Three-dimensional PET emission scan registration and transmission scan synthesis," *IEEE Transactions on Medical Imaging*, vol. 16, no. 5, pp. 542–561, 1997.

[12] J. Martin, A. Pentland, S. Sclaroff, and R. Kikinis, "Characterization of neuropathological shape deformations," *IEEE Transactions on Pattern Analysis and Machine Intelligence*, vol. 20, no. 2, pp. 97–112, 1998.

[13] C. Nikou, F. Heitz, and J. P. Armspach, "Robust registration of dissimilar single and multimodal images," in *Lecture Notes in Computer Science. Proceedings of the 5^{th} European Conference on Computer Vision (ECCV'98)*, Springer-Verlag, Ed., Freiburg, Germany, 2-6 June 1998, vol. 2, pp. 51–65.

[14] C. Nikou, J. P. Armspach, F. Heitz, I.J. Namer, and D. Grucker, "MR/MR and MR/SPECT registration of brain images by fast stochastic optimization of robust voxel similarity measures," *Neuroimage*, vol. 8, no. 6, pp. 30–43, 1998.

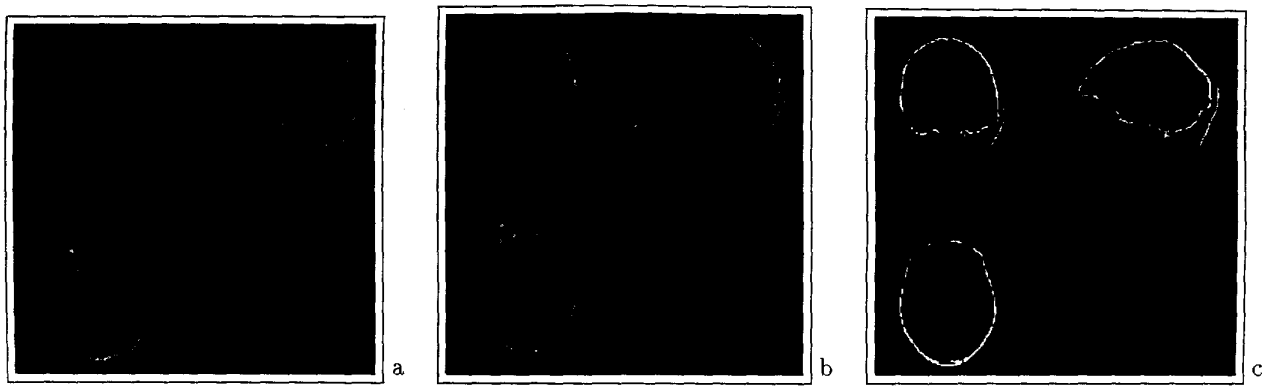

Figure 2: **(a)** *A patient's MR image.* **(b)** *The Canny-Deriche contours of the MRI in (a).* **(c)** *The contour map in (a) after hysteresis thresholding with connected components analysis.*

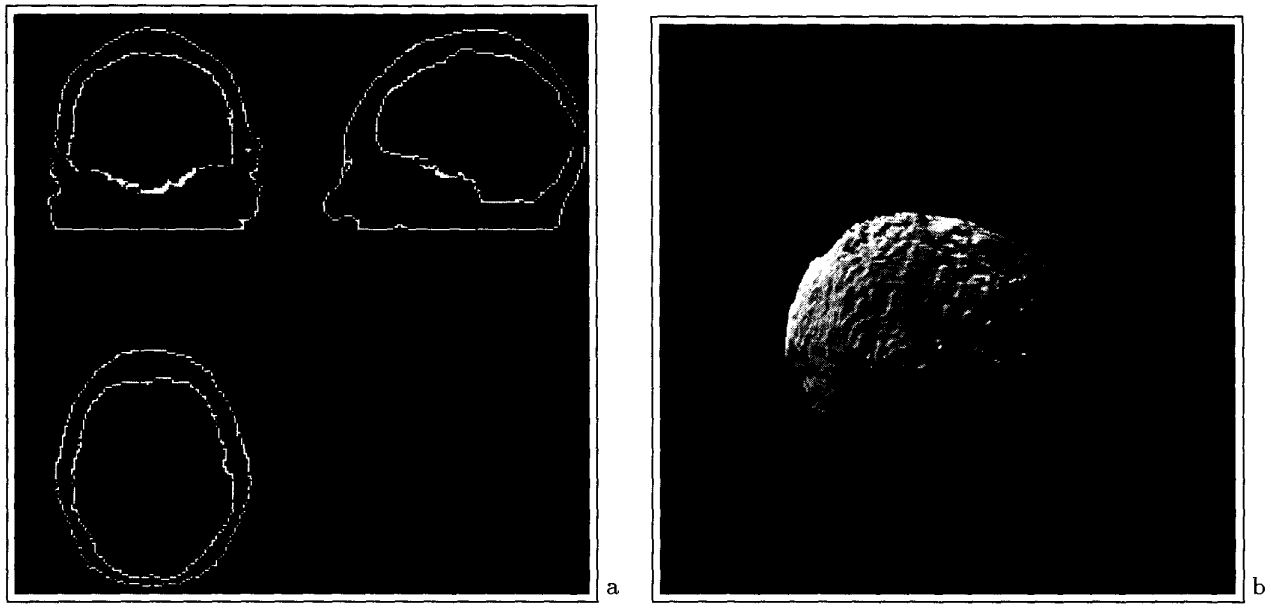

Figure 3: *Brain segmentation.* **(a)** *The MRI volume with the resulting deformable multimodel superimposed are presented in multiplanar view.* **(b)** *The segmented brain surface in 3D visualization.*

[15] N. Otsu, "A threshold selection method from grey-level histograms," *IEEE Transactions on Systems, Man and Cybernetics*, vol. 9, no. 1, pp. 62–66, 1979.

[16] O. Musse, J. P. Armspach, I. J. Namer, F. Heitz, F. Hennel, and D. Grucker, "Data-driven curvilinear reconstruction of 3D MRI: application to cryptogenic extratemporal epilepsy," *Magnetic Resonance Imaging*, vol. 16, no. 7, 1998, To appear (in press).

[17] G. Borgefors, "On digital distance transforms in three dimensions," *Computer Vision and Image Understanding*, vol. 64, no. 3, pp. 368–376, 1996.

[18] K. J. Bathe, *Finite element procedures*, Prentice Hall, Englewood Cliffs, New Jersey, 1996.

[19] A. Pentland and S. Sclaroff, "Closed-form solutions for physically-based shape modeling and recognition," *IEEE Transactions on Pattern Analysis and Machine Intelligence*, vol. 13, no. 7, pp. 730–742, 1991.

[20] C. Nastar, B. Moghaddam, and A. Pentland, "Flexible images: matching and recognition using learned deformations," *Computer Vision and Image Understanding*, vol. 65, no. 2, pp. 179–191, 1997.

[21] O. Monga and R. Deriche, "3D edge detection using recursive filtering," *Computer Vision and Image Understanding*, vol. 53, no. 1, pp. 76–87, 1991.